Paramagnetic Bis(1,4-di-*tert*-butyl-1,4-diazabutadiene) Adducts of Lithium, Magnesium, and Zinc

Michael G. Gardiner,† Graeme R. Hanson,‡ Mark J. Henderson,† Fu Chin Lee,† and Colin L. Raston*,†

Faculty of Science and Technology, Griffith University, Nathan, Brisbane, Queensland 4111, Australia, and Centre for Magnetic Resonance, University of Queensland, St. Lucia, Queensland 4072, Australia

Received September 1, 1993®

Treatments of activated magnesium and zinc, M*, in THF and of sonified bulk lithium in hexane with 1,4-di-*tert*-butyl-1,4-diazabutadiene (Bu^t_2DAB) afford $[M(Bu^t_2DAB)_2]$ as triplet, ligand-centered biradicals in the solid state and at low temperature in solution (M = Mg (**1**) (previously studied using EPR), Zn (**2**)) or a ligand-centered radical (M = Li (**3**) (g_{av} = 2.0034 in hexane, $a(^{14}N\times2)$ = 4.66 × 10^{-4} cm^{-1}, $a(^1H\times2)$ = 4.90 × 10^{-4} cm^{-1}, $a(^7Li)$ = 1.36 × 10^{-4} cm^{-1})). Reaction of M^*/MH_2 with Bu^t_2DAB in THF also gives **1** and **2**, as do the reactions of $MgCl_2$ and $ZnCl_2$ with **3**, and the reaction of **1** with $ZnCl_2$ affords **2**. The room-temperature EPR spectrum of **2** displays two signals attributed to cation/anion ligand-centered radicals, $[M(Bu^t_2DAB)_2]^+[M(Bu^t_2DAB)_2]^-$ (g_{av} (1) = 2.0068, $a(^{14}N\times2)$ = 4.66 × 10^{-4} cm^{-1}, $a(^1H\times2)$ = 6.23 × 10^{-4} cm^{-1}, g_{av} (2) = 2.0077, $a(^{14}N\times2)$ = 4.66 × 10^{-4} cm^{-1}, $a(^1H\times2)$ = 6.23 × 10^{-4} cm^{-1}). At low temperature a dipole–dipole-coupled spectrum is observed, affording a distance of 4.75 Å between the electrons each centered on a Bu^t_2DAB ligand. In the solid state **1** and **2** have *mm* crystallographic symmetry, with mainly angular distortions from regular tetrahedral geometry at the metal centers, M–N = 2.070(7), 2.067(7) Å, (**1**), 1.999(4), 2.013(4) Å, (**2**), N–M–N = 82.1(3), 82.4(3)° (**1**), 84.8(2), 84.7(2)° (**2**), whereas **3** has angular and bond distance tetrahedral distortions, in accordance with the metal center being bound by a radical anion bidentate ligand, Li–N(mean) = 1.995 Å (N–Li–N = 88.3(3)°), and a neutral bidentate ligand, Li–N(mean) = 2.141 Å (N–Li–N = 79.5(2)°). Crystal data (Mo Kα, λ = 0.710 69 Å): **1**, orthorhombic, space group *Ibmm*, a = 12.063(1) Å, b = 14.266(2) Å, c = 14.252(3) Å, V = 2452.8(7) Å^3, Z = 4, R = 0.051; **2**, orthorhombic, space group *Ccmm*, a = 12.388(3) Å , b = 14.225(3) Å, c = 13.705(1) Å, V = 2415.2(8) Å^3, Z = 4, R = 0.036; **3**, monoclinic, space group $P2_1/c$, a = 11.671(7) Å, b = 10.598(1) Å, c = 20.026(1) Å, β = 104.60(3)°, V = 2397(2) Å^3, Z = 4, R = 0.056.

Introduction

Alkaline earth metals activated as amalgams react with 1,4-di-*tert*-butyl-1,4-diazabutadiene (Bu^t_2DAB) to yield solutions containing triplet biradicals $[M(Bu^t_2DAB)_2]$ (M = Mg, Ca, Sr), which have been studied using EPR spectroscopy.[1,2] A reaction between zinc/mercury amalgam and Bu^t_2DAB has been noted, but no EPR data have been reported.[1] The magnesium compound has also been isolated from solution using bulk metal in the presence of magnesium chloride (no yield given),[3] and the analogous zinc species is possibly generated electrochemically.[4] The structural model which is most consistent with the EPR data for M = Mg, Ca, and Sr has the diazabutadiene planes orthogonal, D_{2d} symmetry, with the spin density mainly ligand centered and the metal centers divalent. Even so, a planar model with D_{2h} symmetry has not been ruled out[1] since none of these species have been isolated and structurally authenticated. Radical anion species based on magnesium and zinc attached to one 1,4-diazabutadiene ligand have been generated in solution electrochemically[4] and chemically *via* the reaction of metal dialkyls with the diazabutadiene.[5]

Activated forms of group 13 elements also react with Bu^t_2DAB, yielding species with two chelating ligands $[M(Bu^t_2DAB)_2]$ (M = Al,[6,7] Ga[8,9]). These have been structurally characterized using X-ray diffraction data,[6,8] revealing distorted tetrahedral metal centers associated with geometrically distinct ligands. EPR[6,8,10] and photoelectron spectroscopy (PES)[7] are consistent with one ligand acting as a reduced dianion and the other as a singly reduced radical anion, and thus the presence of Al(III) and Ga(III) species. However, X-ray photon electron spectroscopy (solid) and low-temperature EPR anisotropy for the gallium compound in tetrahydrofuran suggest a significant spin density on the metal center.[11]

Herein we report the synthesis of $[M(Bu^t_2DAB)_2]$ (M = Mg (**1**), and Zn (**2**)) using highly activated metal and their characterization using EPR and X-ray diffraction data. The resulting structural determinations are the first for $[M(Bu^t_2DAB)_2]$ species for the group 2 and 12 elements. This allows a useful comparison with the foregoing group 13 examples which possess one additional electron (M = Mg *vs* Al and Zn *vs* Ga). The reactions of metal hydrides of zinc and magnesium with Bu^t_2DAB have also been investigated as an alternative route to the same compounds, noting that mixtures of metal powder and $LiMH_4$ yield $[M(Bu^t_2DAB)_2]$ (M = Al, Ga).[8,9] These reagents seemingly deliver activated metal, albeit under highly reducing conditions. Also included for comparison are the synthesis and structural elucidation of a group 1 complex of the type $[M(Bu^t_2DAB)_2]$ (M = Li (**3**)) and its utility in preparing **1** and **2** from metal halide salts. This compound is an example where one of the ligands can

† Griffith University.
‡ University of Queensland.
® Abstract published in *Advance ACS Abstracts,* April 15, 1994.

(1) Corvaja, C.; Pasimeni, *Chem. Phys. Lett.* **1976**, *39*, 261.
(2) The International EPR Society is adopting and recommending that "EPR" rather than "ESR" be used to describe this technique.
(3) Clopath, P.; von Zelewsky, A. *Helv. Chim. Acta* **1973**, *56*, 980.
(4) Richter, S.; Daul, C.; von Zelewsky, A. *Inorg. Chem.* **1976**, *15*, 943.
(5) Kaupp, M.; Stoll, H.; Preuss, H.; Kaim, W.; Stahl, T.; van Koten, G.; Wissing, E.; Smeets, W. J. J.; Spek, A. *J. Am. Chem. Soc.* **1991**, *113*, 5606.
(6) Cloke, F. G. N.; Dalby, C. I.; Henderson, M. J.; Hitchcock, P. B.; Kennard, C. H. L.; Lamb, R. N.; Raston, C. L. *J. Chem. Soc., Chem. Commun.* **1990**, 1394.
(7) Cloke, F. G. N.; Dalby, C. I.; Daff, P. J.; Green, J. C.; *J. Chem. Soc., Dalton Trans.* **1991**, 181.
(8) Cloke, F. G. N.; Hanson, G. R.; Henderson, M. J.; Hitchock, P. B.; Raston, C. L. *J. Chem. Soc., Chem. Commun.* **1989**, 1002.
(9) Henderson, M. J.; Kennard, C. H. L.; Raston, C. L.; Smith, G. *J. Chem. Soc. Chem. Commun.* **1990**, 1203.
(10) Kaim, W.; Matheis, W. *J. Chem. Soc., Chem. Commun.* **1991**, 597.
(11) Hanson, G. R.; Henderson, M. J.; Raston, C. L. Unpublished results. The EPR spectrum of the gallium complex recorded in THF at 120 K reveals anisotropy in the **g** and Ga hyperfine matrices.

0020-1669/94/1333-2456$04.50/0

in principle be considered as a singly reduced radical anion, the other simply acting as a neutral bidentate moiety. We focused on lithium because two Bu^t_2DAB ligands are likely to coordinatively saturate the metal center by bonding exclusively through the N centers and also because for the heavier group 1 elements purely ionic structures may lead to different metal–ligand interactions, including polyhapto structures. It is noteworthy that while alkali metals readily react with Bu^t_2DAB,[12,13] yielding either singly or doubly reduced species, none has been isolated and characterized, although a doubly reduced lithium complex has been established for an aryl substituted diazabutadiene, $Li_2(THF)_4[\{\mu\text{-}N(o\text{-tolyl})C(Ph)\}_2]$ (THF = tetrahydrofuran).[14]

Experimental Section

Materials and Methods. 1,4-Di-*tert*-butyl-1,4-diazabutadiene was prepared according to the literature.[15] All reactions were carried out under argon using standard Schlenk and glovebox techniques. Hexane and diethyl ether were dried over Na/K and used immediately; benzene-d_6 was dried over sodium. NMR and mass spectra were recorded on Bruker WM-360 and Kratos MS80 spectrometers. EPR spectra were recorded on a Bruker ER 200D spectrometer at the University of Queensland. The spectrometer was equipped with a Bruker ER035M gaussmeter and an EIP548A microwave frequency counter for the calibration of the magnetic field and the microwave frequency, respectively. Isotropic ($S = {}^1/_2$) and dipole–dipole-coupled spectra were simulated with the computer programs EPR50FIT[16] and GNDIMER[17] on a SUN SPARC Station 10. Electronic absorption spectra were recorded on a Varian DMS 90 UV/vis spectrometer. C, H, and N analysis was performed by the Canadian Microanalytical Services Ltd. Compound **1** has been prepared using $Mg/MgCl_2$/DME mixtures.[3]

Synthesis of $[Mg(Bu^t_2DAB)_2]$ (1). Method a. Highly activated magnesium (0.14 g, 5.76 mmol) was added to a stirred THF solution (30 mL) of sublimed Bu^t_2DAB (1.88 g, 11.17 mmol) at room temperature. After 1 day of stirring a deep green paramagnetic solution was obtained. Unreacted metal was filtered off and solvent removed *in vacuo* to give a deep brown solid. The product recrystallized from hexane to afford deep red crystals (0.24 g, 11.5%): mp 143 °C, g_{av} = 2.0033 (toluene); ^{1}H NMR (360 MHz, benzene-d_6) δ –8.33 (b, Me, $W_{1/2}$ *ca.* 1500 Hz); MS *m/e* 360 (M^+, 16%); IR ν (cm^{-1}) C=N 1630; UV λ_{max} (nm) 224, 284. Anal. Calcd for $C_{20}H_{40}N_4Mg$: C, 66.55; H, 11.19; N, 15.53. Found: C, 65.32; H, 11.00; N, 15.03.

Method b. To a slurry of $MgCl_2$ (0.25 g, 2.63 mmol) in THF (20 mL) was added a THF solution (20 mL) of **3** (1.80 g, 5.25 mmol) over 10 min at –100 °C. On warming to *ca.* 20 °C, the orange solution turned green, and after 2 h solvent and Bu^t_2DAB were removed *in vacuo* at 40 °C. The title compound was then sublimed from the residue under high vacuum (10^{-4} mbar) at 110 °C (0.72 g, 76%).

Synthesis of $[Zn(Bu^t_2DAB)_2]$ (2). Method a. Rieke's zinc (0.55 g, 8.44 mmol) was added to a stirred THF solution (30 mL) of sublimed Bu^t_2DAB (2.83 g, 16.83 mmol) at –80 °C. The reaction mixture was then stirred for 12 h at room temperature to afford a deep green paramagnetic solution. Volatiles were removed *in vacuo*, and the resulting deep brown solid was sublimed at 110 °C (3 mbar) to give deep red/brown crystals (0.45 g, 26.4% yield): mp 140 °C; g_{av} =2.0032 (toluene); ^{1}H NMR (360 MHz, benzene-d_6) δ –10.10 (b, Me, $W_{1/2}$ *ca.* 500 Hz); MS *m/e* 400 (M^+, 16%); IR: ν (cm^{-1}) C=N 1630; UV λ_{max} (nm) 225, 285. Anal. Calcd for $C_{20}H_{40}N_4Zn$: C, 59.75; H, 10.05; N, 13.94. Found: C, 59.05; H, 9.52; N, 13.79.

Method b. To a slurry of $ZnCl_2$ (0.36 g, 2.63 mmol) in THF (20 mL) was added a THF solution (20 mL) of **3** (1.80 g, 5.25 mmol) over 10 min at –100 °C. On warming to *ca.* 20 °C, the orange solution turned green, and after 2 h solvent and Bu^t_2DAB were removed *in vacuo* at 40 °C. The title compound was then sublimed from the residue under high vacuum (10^{-4} mbar) at 100 °C (0.74 g, 71%).

Scheme 1

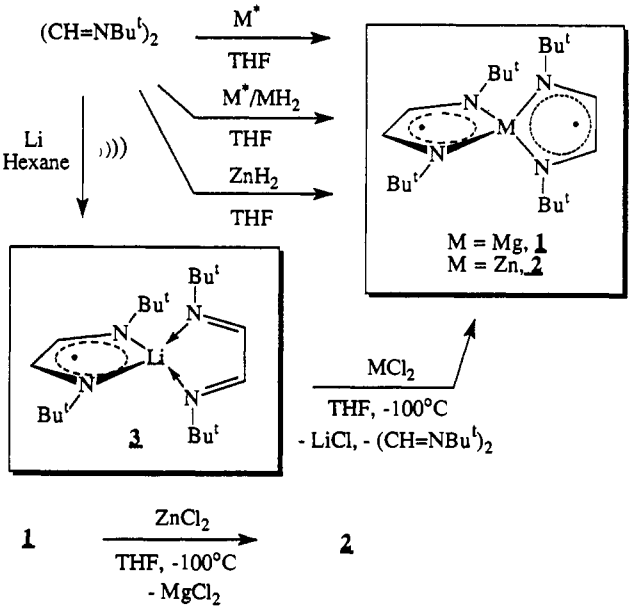

Method c. To a slurry of $ZnCl_2$ (0.25 g, 1.85 mmol) in THF (10 mL) was added a THF solution (10 mL) of **1** (0.63 g, 1.75 mmol) over 5 min at –100 °C. On warming to *ca.* 20 °C, the resulting green solution was left for 12 h. The solvent was then removed *in vacuo*, and the title compound was sublimed from the residue under high vacuum (10^{-4} mbar) at 100 °C (0.41 g, 59%).

Synthesis of $[Li(Bu^t_2DAB)_2]$ (3). Freshly cut lithium (0.10 g, 14.4 mmol) was added to a hexane solution (20 mL) of sublimed Bu^t_2DAB (0.85 g, 5.05 mmol) at room temperature. The resulting mixture was sonicated (40 W) for 2 h to afford a deep brown paramagnetic solution. Concentration *in vacuo* to (*ca.* 5 mL) and cooling to –30 °C yielded dark green crystals (0.78 g, 90% yield): mp 119–121 °C dec; g_{av} = 2.0034 (hexane). Anal. Calcd for $C_{20}H_{40}N_4Li$: C, 69.96; H, 11.74; N, 16.31. Found: C, 68.86; H, 11.68; N, 16.01.

Crystal Structure Determinations. Diffraction data were collected on a Enraf-Nonius CAD4 diffractometer with crystals mounted in capillaries; $2\theta_{max}$ = 40, 60, 50° for **1**, **2**, **3**, respectively, for 2469, 1217, 4415 unique reflections yielding 411, 952, 2053 observed reflections with $I > 3\sigma(I)$ (**1**, **2**) and $I > 2.5\sigma(I)$ (**3**) (no absorption corrections). The structures were solved by direct methods and refined by minimizing $\Sigma w\Delta^2$ with full-matrix least-squares calculations using unit weights and with non-hydrogen atoms anisotropic. The hydrogen atoms (x, y, z; U_{iso}) were included as invariants, except the hydrogens attached to the ring carbons in **3**, which were refined positionally. No extensive, significant extinction effects were found. Neutral-atom complex scattering factors[18] were employed; computation used the XTAL program system,[19] implemented on a SUN SPARC Station 2. Molecular core geometries, atom coordinates, and crystal data are given in Figures 4 and 5 and Tables 2–5.

Discussion

The synthesis of compounds **1–3** are shown in Scheme 1. For **1** and **2** derived directly from Bu^t_2DAB, activated forms of the metal, M*, were required, and then only for low yields of the products; with bulk metal there was no noticeable reaction over several days. Activated metals used initially were magnesium powder (derived from the condensation of metal in hexane) and Rieke's zinc.[20] Compound **3** was conveniently prepared in high yield in hexane using bulk metal and the application of sonic

(12) Tom Dieke, H.; Franz, K.-D. *Angew. Chem., Int. Ed. Engl.* **1975**, *14*, 269.
(13) Scolz, J.; Richter, B.; Goddard, R.; Kruger, C. *Chem. Ber.* **1993**, *126*, 57.
(14) Herrmann, W. A.; Denk. M.; Behm, J.; Scherer, W.; Klingan, F.-R.; Bock, H.; Solouki, B.; Wagner, M. *Angew. Chem., Int. Ed. Engl.* **1992**, *31*, 1485.
(15) Kliegman, J. M.; Barnes, R. K. *Tetrahedron* **1970**, *26*, 2555.
(16) Ang, H. G.; Kwik, W. L.; Hanson, G. R.; Crowtler, J. A.; McPartlin, M.; Choi, N. *J. Chem. Soc., Dalton Trans.* **1991**, 3139.
(17) Smith, T. D.; Pilbrow, J. R. *Coord. Chem. Rev.* **1974**, *13*, 173.
(18) *International Tables for X-ray Crystallography*; Ibers, J. A., Hamilton, W. C., Eds.; Kynoch Press: Birmingham, England, 1974; Vol. 4.
(19) *XTAL User's Manual—Version 3.0*; Hall, S. R., Stewart, J. M., Eds.; Universties of Western Australia and Maryland: Nedlands and College Park, 1990.
(20) Rieke, R. D.; Li, P. T. J.; Burns, T. P.; Uhm, S. T. *J. Org. Chem.* **1981**, *46*, 4323.

energy (40 W). Lithium hydride failed to react with Bu^t_2DAB in hexane, unlike zinc hydride (see below).

Direct condensation of magnesium with Bu^t_2DAB was also attempted but with no improvement in yield. The synthesis of the related aluminum and gallium compounds, **4** and **5**, respectively, also required activated metal, either as metal vapors[5,9] or as mixtures of metal powder and $LiMH_4$.[7,9] In the present study we also explored the possibility of using metal/metal hydride mixtures and metal hydrides to improve the yields of **1** and **2**, but to no avail. For the combinations $Mg^*/MgH_2/Bu^t_2DAB$ and Zn^*/ZnH_2[21]$/Bu^t_2DAB$ in THF at ambient temperature, compounds **1** and **2** were isolated in yields comparable to that for M*. In the case of Li_2ZnH_4[22]$/Bu^t_2DAB$ in THF, and the same combination with Zn*, an intractable paramagnetic compound was formed. There was no apparent reaction for the mixture MgH_2/Bu^t_2DAB in THF, even under reflux, whereas ZnH_2/Bu^t_2DAB in THF overnight at 50 °C gave **2** in a yield comparable to those of the foregoing methods. Under such conditions, ZnH_2 is unstable,[23] decomposing to metal and hydrogen, and presumably the formation of M* precedes electron transfer. Reasonable yields of **1** and **2** were obtained by metathetical exchange involving the group 2/12 chloride and compound **3**, with the excess Bu^t_2DAB readily removed *in vacuo*. Similarly, compound **2** can be prepared from compound **1** and $ZnCl_2$ (Scheme 1).

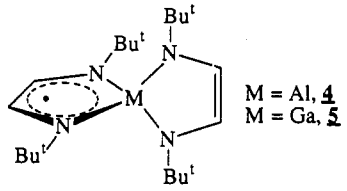

M = Al, **4**
M = Ga, **5**

Compounds **1–3** rapidly decompose in air and are stable indefinitely at room temperature: **1** and **2** sublime *in vacuo* at 110 and 100 °C, respectively, at *ca.* 3 mbar, and **3** decomposes above 119 °C. An earlier report on the electrochemical generation of **1** claimed the species has a low stability.[3,4] Characterization of **1–3** rests on microanalyses, crystal structure determinations (see below), and EPR data which in the case of **1** are already available in the literature.[1]

The EPR spectra of **1** and **2** were recorded in hexane and THF and are similar to that for **1** in 2-MeTHF;[1,3] EPR spectra of **2** and **3** are given in Figures 1–3. The frozen-solution spectrum of **2** (Figure 1a) indicates that this complex is a biradical with an electron localized on each ligand, the ligands being orthogonal to each other. The EPR spectrum can be described as either a triplet spectrum with the spin Hamiltonian[17]

$$\mathbf{H} = S\cdot D\cdot S + g\beta B\cdot S$$

or as the spectrum of a species in which the electrons are dipole–dipole coupled[17]

$$\mathbf{H} = \sum_{i=1,2} \mathbf{g}_i\beta B_i\cdot S_i + \mathbf{H}_{dip}$$

$$\mathbf{H}_{dip} = \frac{\mu_1\cdot\mu_2}{r^3} - \frac{3(\mu_1\cdot r)(\mu_2\cdot r)}{r^5} = S_1\cdot J\cdot S_2$$

where D is the zero-field splitting, S the electron spin, $\mathbf{g}$ the $\mathbf{g}$ matrix, β the Bohr magneton, B the magnetic field, μ the magnetic moment of the electron, r the distance between the electrons, and J the exchange coupling tensor. Both J and D are second rank tensors and cannot be distinguished when r is short. Using the dipole–dipole approach, with $\mathbf{H}_1 = \mathbf{H}_2$, $g_{iso} = 2.000$, and a distance of 4.75 ± 0.2 Å between the two electrons yields the simulation shown in Figure 1b. This corresponds to a value of $D = 2.31 \times 10^{-2}$ cm^{-1} measured from the spectrum.

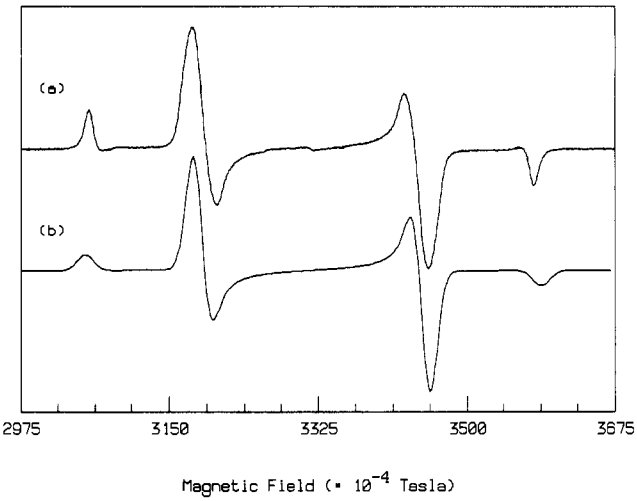

Figure 1. Frozen-solution EPR spectra of $[Zn(Bu^t_2DAB)_2]$ (**2**) recorded in THF at 120 K: (a) experimental spectrum, ν = 9.2986 GHz; (b) computer simulation, LSE = 4.879×10^{-3} (LSE = $\sum_{i=1}^{n} (E_i/I_E - S_i/I_S)^2/n$, where I_E and I_S are the normalized factors (doubly integrated intensities) and n is the number of points in both simulated (S) and experimental (E) spectra).

Table 1. Isotropic g, A(M), $A(^{14}N)$, and $A(^1H)$ Values for $[M(Bu^t_2DAB)_2]$ Species

metal (M)	compd	g_{av}	A_{av}(M)[a]	A_{av}(N)[a]	A_{av}(H)[a]	ref
Mg	**1**	2.0036				3
Zn	**2a**	2.0068	*b*	4.66 (2)[c]	6.23 (2)[c]	This work
	2b	2.0077	*b*	4.66 (2)[c]	6.23 (2)[c]	This work
^{7}Li	**3**	2.0034	1.36 (1)[c]	4.66 (2)[c]	4.90 (2)[c]	This work
^{27}Al	**4**	2.0012	5.0 (1)[c]	5.0 (2)[c]	5.0 (2)[c]	6, 10
^{69,71}Ga	**5**	2.0024	18.39 (1)[c]	2.64 (4)[c]		9

[a] Hyperfine coupling constants reported in units of 10^{-4} cm^{-1}. [b] Could not be determined. [c] Figures in parentheses show the number of magnetically equivalent nuclei.

A comparison of $r/2$ (2.37 Å) with the length of the vectors (a, b) determined from the X-ray structure (see below) is consistent

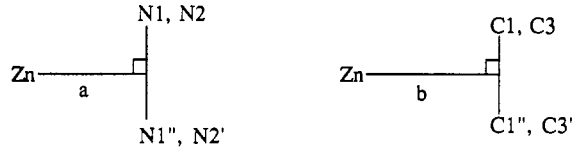

a = 1.48, 1.49 Å b = 2.63, 2.65 Å

with the electron being delocalized around the N_2C_2 backbone. This is as expected from the magnitude of the nitrogen and proton hyperfine coupling constants observed for the $S = {}^1/_2$ species discussed below (Table 1).

Raising the temperature to 298 K produces an isotropic EPR signal centered around $g \approx 2$, which is similar to that found in the EPR spectrum of compound **1**.[3] The absence of the dipole–dipole-coupled (triplet-state) EPR spectrum indicates that this species has a short spin–lattice relaxation time, T_1. In dilute solution (*ca.* 10^{-4} *M*) the EPR spectrum of **2**, Figure 2a, reveals the presence of two components, labeled **2a** and **2b**. The increased resolution in this spectrum can be attributed to the elimination of intermolecular dipole–dipole coupling at higher temperatures.

(21) Synthesis of ZnH_2: variation of published procedure, *viz.* treating diethylzinc with H_3AlNMe_3 rather than AlH_3 (Ashby, E. C.; Watkins, J. J. *Inorg. Synth.* **1977**, *17*, 6).
(22) Ashby, E. C.; Watkins, J. J. *Inorg. Chem.* **1973**, *12*, 2493.
(23) Bluke, R.; Breicis, V.; Belicka, B.; Liepina, L. *Latv. PSR Zinat. Akad. Vestis, Kim. Ser.* **1971**, *1*, 23.
(24) van Koten, G.; Jastrzebski, J. T. B. H.; Vrieze, K. *J. Organomet. Chem.* **1983**, *250*, 49.

Table 2. Crystal Data for [M(Bu$^t_2$DAB)$_2$] (M = Mg (**1**), Zn (**2**), Li (**3**))

1: $C_{20}H_{40}N_4Mg$	fw 360.95
a = 12.063(1) Å	space group *Ibmm* (No. 74)
b = 14.266(2) Å	T = 25 °C
c = 14.252(3) Å	λ = 0.710 73 Å
V = 2452.8(7) Å^3	ρ_{calcd} = 0.977 g cm^{-3}
Z = 4	μ = 0.86 cm^{-1}
	R^a = 0.051
2: $C_{20}H_{40}N_4Zn$	fw 401.90
a = 12.388(3) Å	space group *Ccmm* (No. 63)
b = 14.225(3) Å	T = 25 °C
c = 13.705(1) Å	λ = 0.710 73 Å
V = 2415.2(8) Å^3	ρ_{calcd} = 1.105 g cm^{-3}
Z = 4	μ = 10.57 cm^{-1}
	R^a = 0.036
3: $C_{20}H_{40}N_4Li$	fw 343.50
a = 11.671(7) Å	space group $P2_1/c$ (No. 14)
b = 10.598(1) Å	T = 24 °C
c = 20.026(1) Å	λ = 0.710 73 Å
β = 104.60(3)°	ρ_{calcd} = 0.952 g cm^{-3}
V = 2397(2) Å^3	μ = 0.61 cm^{-1}
Z = 4	R^a = 0.056

^{a} $R = \Sigma||F_o| - |F_c||/\Sigma|F_o|$.

Table 3. Atom Positional and Isotropic Equivalent Thermal Parameters for [Mg(Bu$^t_2$DAB)$_2$] (**1**)

	x/a	y/b	z/c	U^a
Mg	0.6252(3)	$^1/_4$	$^1/_2$	0.045(1)
N(1)	0.4958(5)	$^1/_4$	0.4046(4)	0.051(2)
N(2)	0.7538(5)	0.1548(4)	$^1/_2$	0.050(2)
C(1)	0.4007(6)	$^1/_4$	0.4506(5)	0.053(3)
C(2)	0.4948(8)	$^1/_4$	0.3012(6)	0.066(3)
C(21)	0.613(1)	$^1/_4$	0.2698(6)	0.121(6)
C(22)	0.4357(7)	0.3377(6)	0.2651(5)	0.131(4)
C(3)	0.8495(6)	0.2008(5)	$^1/_2$	0.054(3)
C(4)	0.7563(8)	0.0512(5)	$^1/_2$	0.067(3)
C(41)	0.636(1)	0.0200(6)	$^1/_2$	0.117(6)
C(42)	0.8146(7)	0.0142(5)	0.5883(6)	0.136(4)

^{a} Equivalent isotropic U (Å^2) defined as one-third of the trace of the orthogonalized U_{ij} tensor.

Table 4. Atom Positional and Isotropic Equivalent Thermal Parameters for [Zn(Bu$^t_2$DAB)$_2$] (**2**)

	x/a	y/b	z/c	U^a
Zn	0.14699(7)	$^1/_2$	$^1/_4$	0.0435(3)
N(1)	0.0278(3)	0.5947(3)	$^1/_4$	0.049(1)
N(2)	0.2671(3)	$^1/_2$	0.3490(3)	0.049(1)
C(1)	−0.0652(4)	0.5492(4)	$^1/_4$	0.054(2)
C(2)	0.0278(5)	0.6988(4)	$^1/_4$	0.066(2)
C(21)	0.1460(7)	0.7289(4)	$^1/_4$	0.101(3)
C(22)	−0.0267(5)	0.7366(3)	0.1583(4)	0.112(2)
C(3)	0.3607(4)	$^1/_2$	0.3003(3)	0.054(2)
C(4)	0.2621(5)	$^1/_2$	0.4567(3)	0.058(2)
C(41)	0.1443(6)	$^1/_2$	0.4842(4)	0.111(3)
C(42)	0.3143(5)	0.4128(4)	0.4981(4)	0.125(3)

^{a} Equivalent isotropic U (Å^2) defined as one-third of the trace of the orthogonalized U_{ij} tensor.

The components **2a** and **2b** may arise either from the presence of two species in solution or from the same molecule in which the two Bu$^t_2$DAB ligands are orientated in such a way as to eliminate (reduce to zero) the dipole–dipole interaction.

Computer simulations of the two components with the fortran program EPR50FIT are shown in Figure 2(b,c with the isotropic g and A values listed in Table 1. Figure 2d shows the spectrum obtained by adding spectra b and c of Figure 2 in equal proportions. An examination of the EPR parameters for **2a** and **2b** (Table 1) reveals only subtle changes in g_{av}, which can be attributed to either slight differences in the coordination of the two Bu$^t_2$DAB ligands to the zinc ion or the presence of cation and anion radicals in solution. The latter is more likely as differences in the coordination of the Bu$^t_2$DAB ligands to the zinc ion would be

Table 5. Atom Positional and Isotropic Equivalent Parameters for [Li(Bu$^t_2$DAB)$_2$] (**3**)

	x/a	y/b	z/c	U^a
Li	0.3005(5)	0.2593(6)	0.3701(3)	0.061(2)
N(1)	0.2793(3)	0.4222(3)	0.3188(2)	0.058(1)
N(4)	0.1916(3)	0.3243(3)	0.4247(2)	0.058(1)
N(5)	0.2884(3)	0.0760(3)	0.3247(2)	0.054(1)
N(8)	0.4742(2)	0.1874(3)	0.4171(2)	0.054(1)
C(1)	0.3158(3)	0.4771(4)	0.2596(2)	0.069(2)
C(2)	0.2129(4)	0.4901(4)	0.3495(2)	0.065(2)
C(3)	0.1683(3)	0.4408(4)	0.4027(2)	0.064(2)
C(4)	0.1355(4)	0.2754(4)	0.4774(2)	0.067(2)
C(5)	0.1882(3)	0.0188(4)	0.2729(2)	0.066(2)
C(6)	0.3823(4)	0.0183(4)	0.3467(2)	0.067(2)
C(7)	0.4833(3)	0.0766(4)	0.3979(2)	0.064(2)
C(8)	0.5732(3)	0.2512(4)	0.4661(2)	0.066(2)
C(11)	0.3839(4)	0.3722(5)	0.2333(2)	0.091(2)
C(12)	0.2078(4)	0.5155(5)	0.2017(2)	0.104(2)
C(13)	0.3976(4)	0.5916(5)	0.2816(3)	0.095(2)
C(41)	0.1856(5)	0.1434(5)	0.4961(3)	0.119(3)
C(42)	0.0018(4)	0.2664(6)	0.4490(3)	0.127(3)
C(43)	0.1635(6)	0.3555(5)	0.5426(3)	0.124(3)
C(51)	0.1011(4)	0.1252(5)	0.2470(3)	0.106(2)
C(52)	0.2295(5)	−0.0381(6)	0.2127(2)	0.115(3)
C(53)	0.1315(4)	−0.0831(5)	0.3077(3)	0.114(3)
C(81)	0.6812(4)	0.1706(5)	0.4955(3)	0.111(2)
C(82)	0.6057(6)	0.3633(6)	0.4281(3)	0.150(3)
C(83)	0.5232(5)	0.2969(6)	0.5253(3)	0.128(3)

^{a} Equivalent isotropic U (Å^2) defined as one-third of the trace of the orthogonalized U_{ij} tensor.

expected to effect changes not only in g but also in the nitrogen and proton coupling constants. In addition a dipole–dipole (triplet-state) spectrum would not be expected to be observed (a flat baseline, as it would have a short T_1). The cationic and anionic radicals are in equilibrium with the dipole–dipole-coupled species (eq 1).

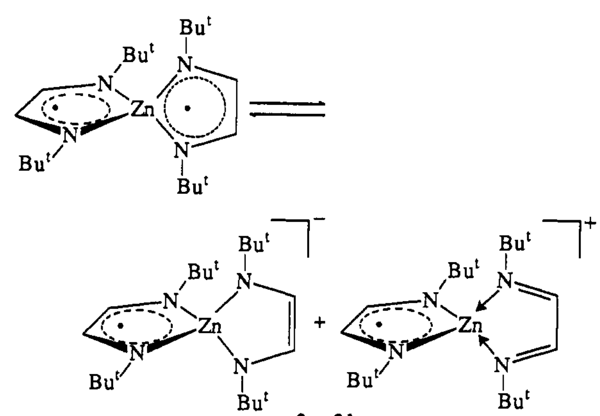

2a, **2b** (1)

Computer simulation of the EPR spectrum of the lithium complex (Figure 3b) reveals hyperfine coupling to two magnetically equivalent ^{14}N nuclei and two magnetically equivalent ^{1}H in addition to ^{7}Li coupling. The magnitude of these parameters (Table 1) indicates the electrons are ligand centered, similar to the case observed for the zinc complex. EPR experiments on ^{6}Li-enriched samples of **3** gave spectra consistent with the simulation of the EPR spectrum of the natural-abundance complex, that is a triplet [$I(^6$Li$)$ = 1] overlayed on the usual pseudoseptet of a ligand centered Bu$^t_2$DAB radical anion. While hyperfine coupling to two magnetically equivalent ^{14}N nuclei and two ^{1}H is observed in the magnesium, zinc, aluminum,[9,10] and lithium complexes, hyperfine coupling to four magnetically equivalent nitrogen nuclei is observed in the gallium complex, **5**.[8] This suggests a dynamic Jahn–Teller distortion in the gallium complex with the unpaired electron jumping between ligands on a time scale comparable with that of the EPR experiments. This is consistent with the greater spin density on the gallium compared

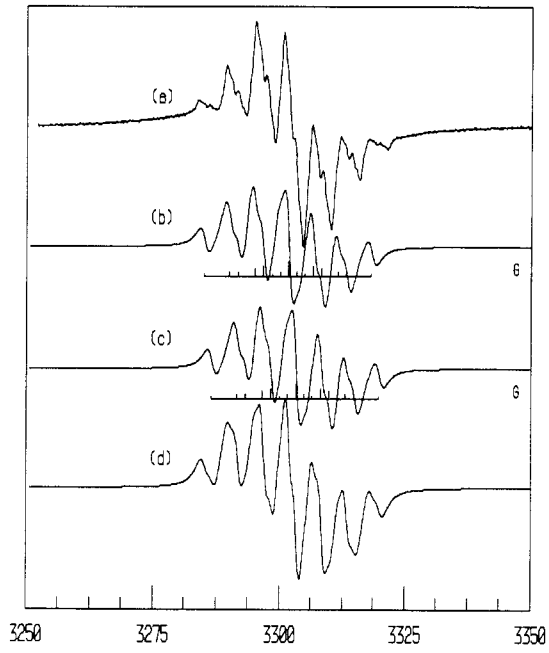

Figure 2. Room-temperature EPR spectra of $[Zn(Bu^t_2DAB)_2]$ (**2**) recorded in THF: (a) experimental spectrum for dilute solutions (*ca.* 10^{-4} M), ν = 9.2777 GHz; (b, c) computer simulations of the two subspectra, labeled as **2a** and **2b** in the text; (d) addition of spectra **2a** and **2b**. LSE = 1.6×10^{-3}.

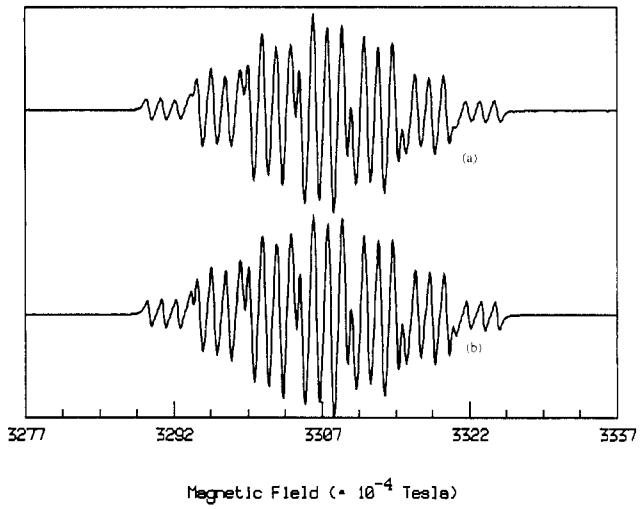

Figure 3. Room-temperature EPR spectrum of $[Li(Bu^t_2DAB)_2]$ (**3**) recorded in hexane (a) and computer simulation of the resonances (b) assuming a single unpaired electron is coupled to two magnetically equivalent ^{14}N, two magnetically equivalent ^1H, and ^7Li (see Table 1).

to other metal ions in the other compounds, *viz.* a lower activation energy for this process than in **1**–**4**. Moreover, greater metal spin density in **5** is consistent with XPS and anisotropic EPR spectra at low temperatures in THF.[11]

Results of the X-ray structure determinations of **1** and **2** are presented in Tables 2–4 and Figure 4. Molecules of **1** and **2** reside on *mm* symmetry sites with the asymmetric unit comprising the metal center and two half ligands. For compound **1** the differences in geometries between each ligand are within three standard deviations of their bond distances and angles (Figure 4), so that the overall symmetry becomes $2mm$ (D_{2d}). In compound **2**, however, there is a pronounced difference between the ligands with Zn–N = 1.999(4) and 2.013(4) Å, $N–C_{ring}$ = 1.321(6) and 1.339(6) Å, and C–C = 1.400(8) and 1.378(7) Å for ligands 1 and 2, respectively. This suggests a slight difference

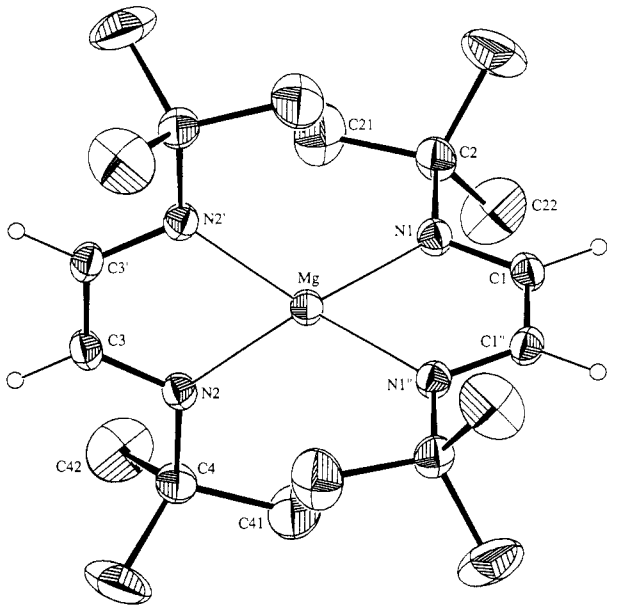

Figure 4. Molecular projection of $[Mg(Bu^t_2DAB)_2]$ (**1**), which is similar to that of $[Zn(Bu^t_2DAB)_2]$ (**2**), showing 20% thermal ellipsoids for non-hydrogen atoms and arbitrary radii for hydrogen atoms shown. Selected bond distances (Å) and angles (deg) are as follows (values in brackets are for $[Zn(Bu^t_2DAB)_2]$ (**2**): M–N(1), 2.070(7) [1.999(4)]; M–N(2), 2.067(7) [2.013(4)]; N(1)–C(1), 1.32(1) [1.321(6)]; N(1)–C(2), 1.47(1) [1.481(7)]; N(2)–C(3), 1.33(1) [1.339(6)]; N(2)–C(4), 1.48(1) [1.478-(6)]; C(1)–C(1)″, 1.41(1) [1.400(8)]; C(3)–C(3)′, 1.40(1) [1.378(7)]; N(1)–M–N(1)″, 82.1(3) [84.8(2)]; N(2)–M–N(2)′, 82.4(3) [84.7(2)]; N(1)–M–N(2), 124.6(1) [123.0(9)]; M–N(1)–C(2), 131.5(6) [131.9(3)]; M–N(1)–C(1) 109.2(5) [108.3(3)]; M–N(2)–C(4), 132.4(5) [130.0(3)]; M–N(2)–C(3), 109.2(5) [107.7(3)]; C(2)–N(1)–C(1), 119.2(7) [119.8(4)]; C(4)–N(2)–C(3), 118.4(7) [122.3(4)]; N(1)–C(1)–C(1)″, 119.7(7) [119.3(5)]; N(2)–C(3)–C(3)′, 119.6(7) [119.9(4)].

in charge density on the ligands, the ligand with the shortest Zn–N distances and the longer $N–C_{ring}$ distance and shorter C–C distance being slightly more reduced. Nevertheless, the difference is small and overall both ligands have geometries within the realms of those for radical anion species bound to metal centers, as for both ligands in compound **1**, which compare well with the singly reduced ligands in **4**[6] and **5**.[8] The origin of the asymmetry in **2** but not in **1** is unclear, but we note that the compounds crystallize in different space groups (*Ibmm*, **1**; *Ccmm*, **2**) even though the metal center site symmetries are the same. Any asymmetry in charge density on the ligands, and thus an induced dipole moment, is likely to affect molecular packing characteristics. In this context, we note that compound **3**, which is viewed as $[Li(Bu^t_2DAB^-)(Bu^t_2DAB)]$ (EPR data; see also below), and **4** and **5**, established as $[M(Bu^t_2DAB^-)(Bu^t_2DAB^{2-})]$,[6-9] crystallize in different space groups again: $P2_1/c$ for **3**, with no crystallographically imposed symmetry on the metal center; and *Pnma* for **4**[6] and **5**[8], which have *m*-metal symmetry.

The differences in mean M–N distances for **1** and **2**, 2.068 and 2.006 Å, reflect the slightly smaller size of zinc relative to magnesium for largely covalent metal–ligand interactions.[5,25,26] In addition, the mean angles subtended at the metal centers, 82.3 and 84.8°, respectively, reflect the smaller size of zinc for the same ligand "bite" in the two compounds. Average geometries for the two chelate rings of each compound are within three standard deviations of their bond distances and angles (Figure 4) and are thus deemed to have similar average ligand charge densities. This finding, coupled with a comparison of metal–N distances (above), is consistent with both **1** and **2** existing as triplet species in the solid state, as for the same species in solution

(25) Shannon, R. D. *Acta Crystallogr.* **1976**, *A23*, 751.
(26) Henderson, M. J.; Papasergio, R. I.; Raston, C. L.; White, A. H.; Lappert, M. F. *J. Chem. Soc., Chem. Commun.* **1986**, 672.

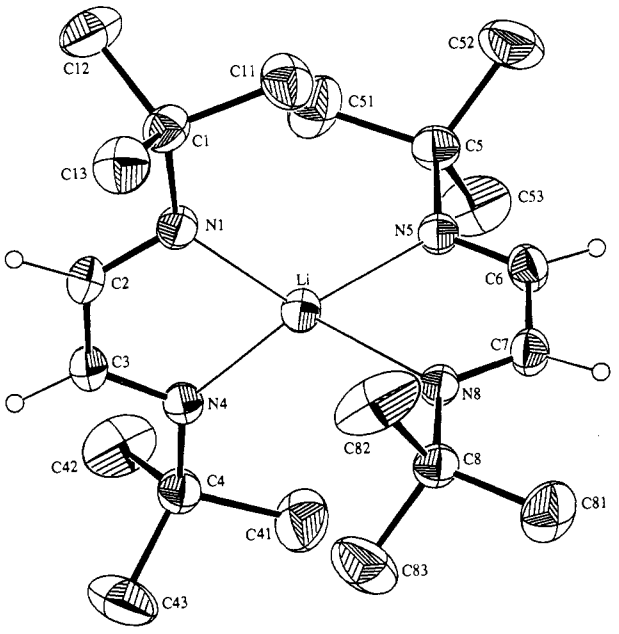

Figure 5. Molecular projection of [Li(Bu$^t_2$DAB)$_2$] (**3**) with 20% thermal ellipsoids for nonhydrogen atoms and arbitrary radii hydrogen atoms shown. Selected bond distances (Å) and angles (deg) are as follows: Li–N(1,4,5,8), 1.993(7), 1.996(8), 2.134(7), 2.148(6); N(1)–C(1), 1.476(6); N(4)–C(4), 1.469(6); N(5)–C(5), 1.483(5); N(8)–C(8), 1.478(4); N(1)–C(2), 1.317(6); N(4)–C(3), 1.317(5); N(5)–C(6), 1.236(5); N(8)–C(7), 1.248(5); C(2)–C(3), 1.399(7); C(6)–C(7), 1.488(5); N(1)–Li–N(4,5,8), 88.3(3), 125.6(3), 120.9(3); N(4)–Li–N(5,8), 124.4(3), 122.9(3); N(5)–Li–N(8), 79.5(2); Li–N(1)–C(1), 137.0(3); Li–N(4)–C(4), 137.1(3); Li–N(5)–C(5), 128.8(3); Li–N(8)–C(8), 128.5(3); Li–N(1)–C(2), 104.1(3); Li–N(4)–C(3), 104.3(3); Li–N(5)–C(6), 109.9(3); Li–N(8)–C(7), 110.1(3); C(1)–N(1)–C(2), 118.8(3); C(3)–N(4)–C(4), 118.7(3); C(5)–N(5)–C(6), 121.3(3); C(7)–N(8)–C(8), 121.5(3); N(1)–C(2)–C(3), 121.7(4); N(4)–C(3)–C(2), 121.4(4); N(5)–C(6)–C(7), 121.2(4); N(8)–C(7)–C(6), 119.2(3).

at low temperature (EPR). The Zn–N distances for **2** are shorter than in [ZnMe$_2$(Bu$^t_2$DAB)], 2.219 Å (mean),[5] as expected for the same chelate ring system but with the ligand now acting as a neutral bidentate donor. Overall, the metal–ligand distances in **1** and **2** are significantly less than distances in four-coordinate compounds of magnesium and zinc where the N centers act as sp^2 donor groups.[26,27] For compound **2**, comparison of the N–Zn–N angle with that in [ZnMe$_2$(Bu$^t_2$DAB)][5] is also informative—[ZnMe$_2$(Bu$^t_2$DAB)] has the lower angle, 75.0(2)°,[5] in accordance with larger M–N distances.

Compound **3** crystallizes with one molecule in the asymmetric unit, which approximates to *mm* metal core symmetry. There is a clear distinction between the two ligands, in both Li–N distances and geometries within the chelate rings which are diagnostic of an electron trapped on one ligand (Li–N(mean) = 1.994 Å, C_{ring}–N (mean) = 1.317 Å, C–C = 1.399(7) Å) and the other ligand simply acting as a neutral bidentate (Li–N(mean) = 2.141 Å , C_{ring}–N(mean) = 1.242 Å, C–C = 1.488(5) Å). Indeed, for the latter, the C_{ring}–N and C–C distances compare favorably with the corresponding distances in [ZnMe$_2$(Bu$^t_2$DAB)].[5] For the same ligand, the Li–N distance is unexceptional for four-coordinate lithium to sp^2 N donor contacts in general.[28] The reduced ligand C_{ring}–N and C–C distances are in close agreement with the corresponding distances in **1** and **2**, and the Li–N distances, are within the range established for monomeric four-coordinate amidolithium species.[28]

In summary, the authenticated structures define a new bonding type for bis(1,4-diazabutadiene)metal species, where both ligands are singly reduced, *viz.* [M(Bu$^t_2$DAB^{-})$_2$] (M = Mg, Zn) in the solid state and in solution at low temperature, and where one ligand is singly reduced, the other acting as a neutral bidentate ligand, *viz.* [Li(Bu$^t_2$DAB^{-})(Bu$^t_2$DAB)]. In addition, we have shown that M*/MH$_2$ mixtures and ZnH$_2$ in THF in the presence of Bu$^t_2$DAB and the lithium complex with magnesium and zinc chloride are effective in forming the magnesium and zinc compounds.

Acknowledgment. We gratefully acknowledge support of this work by the Australian Research Council and thank Colin Kennard and Karl Byriel for collecting the X-ray diffraction data.

Supplementary Material Available: Tables giving atomic positional parameters, thermal parameters, ligand hydrogen parameters, extended metal core geometries, and ligand non-hydrogen geometries (9 pages). Ordering information is given on any current masthead page.

(27) Westerhausen, M.; Rademacher, B.; Schwartz, W. *J. Organomet. Chem.* **1992**, *427*, 275.

(28) E.g.: Barr, D.; Clegg, W.; Mulvey, R. E.; Snaith, R. *J. Chem. Soc., Chem. Commun.* **1984**, 469. Engelhardt, L. M.; Jacobsen, G. E.; Junk, P. C.; Raston, C. L.; Skelton, B. W. *J. Chem. Soc., Dalton Trans.* **1988**, 1011.